Black holes of a general two-dimensional dilaton gravity theory

José P. S. Lemos*
Departamento de Astrofísica, Observatório Nacional-CNPq, Rua General José Cristino 77, 20921 Rio de Janeiro, Brazil and Departamento de Física, Instituto Superior Técnico, Av. Rovisco Pais 1, 1096 Lisboa, Portugal

Paulo M. Sá†
Unidade de Ciências Exactas e Humanas, Universidade do Algarve Campus de Gambelas, 8000 Faro, Portugal
(Received 26 August 1993)

A general dilaton gravity theory in 1+1 spacetime dimensions, with a cosmological constant λ and a new dimensionless parameter ω, contains as special cases the constant curvature theory of Teitelboim and Jackiw, the theory equivalent to vacuum planar general relativity, the first-order string theory, and a two-dimensional purely geometrical theory. The equations of this general two-dimensional theory admit several different black holes with various types of singularities. The singularities can be spacelike, timelike, or null, and there are even cases without singularities. Evaluation of the ADM mass, as a charge density integral, is possible in some situations by carefully subtracting the black hole solution from the corresponding linear dilaton at infinity.

PACS number(s): 04.70.Dy, 04.50.+h, 11.25.Sq

I. INTRODUCTION

Black holes and spacetime singularities are fundamental concepts which have been taken into account in the search for the possible links between general relativity and quantum mechanics. The black hole concept is connected to the nonlocal notion of an event horizon. On the other hand, a spacetime singularity is a concept which is usually associated with unbound values of several physical quantities. Both concepts are not related *a priori*. Yet, in classical general relativity, the existence of a black hole implies the existence of a spacetime singularity. It is conjectured that quantum effects of spacetime will play a role in explaining the singularity as a true quantum object. A possible quantum mechanical framework for general relativity is provided by string theory. Within this theory, black hole solutions have been found for various number of dimensions [1]. These solutions, in turn, allow for the possibility of analyzing the singularity problem from new perspectives. In particular, black hole solutions in two-dimensional (2D) spacetimes have been playing an important role in the understanding of these issues. Indeed, in pertubation theory, the string field equations yield a 2D black hole with spacetime singularities similar to the Schwarzschild metric [2, 3]. In contrast, in the exact conformal quantum field theory [3, 4] it has been shown that the corresponding spacetime is free of singularities [5]. This is welcome since it provides an example where the exact quantum description prevents the formation of a singularity. There are several 2D theories with nontrivial dynamics. One that has been widely studied is the constant curvature theory of Teitelboim and Jackiw [6, 7]. Within this theory one can show that the corresponding black hole is also free of spacetime singularities and with a structure analogous to the exact string solution [8]. A 2D theory, which also has been discussed, is the $R = T$ theory [9, 10]. Another 2D theory, introduced in [11], equivalent to planar general relativity, also admits black hole solutions which, as expected, give rise to spacetime singularities.

In order to see how these features, such as existence or not of singularities and event horizons, might develop from theory to theory, it is important to have a general theory in which the above 2D theories could be connected, each being a special case of the general theory. In this manner, results found in one of the theories could be related straightforwardly with the others. Brans-Dicke theory in 2D provides such a link [11]. The theory is specified by two fields, the dilaton ϕ and the graviton $g_{\mu\nu}$, and two parameters, the cosmological constant λ, and the parameter ω. In this paper we solve and analyze black hole and related solutions for any values of the parameters ω and λ. In order to distinguish black hole solutions from other solutions we have to define properly the notion of black hole event horizon. As it is known [12] one has first to characterize the possibility of escaping to future infinity, which we denote by $\mathcal{J}^+$ (although it does not necessarily mean future null infinity). We then say that the spacetime M contains a black hole if M is not completely contained in the causal past of future infinity denoted by $J^-(\mathcal{J}^+)$. The black hole region is then given by $M - J^-(\mathcal{J}^+)$, whose boundary is defined as being the event horizon. In Sec. II, we set the equations. In Sec. III, we divide the solutions in different classes, depending on the values of the various parameters, and study their causal structure with the corresponding Penrose diagram. In Sec. IV, we calculate the Arnowitt-Deser-Misner (ADM) masses of the solutions. Finally, in Sec. V, we conclude and comment on the links between the solutions.

II. THE EQUATIONS

We propose to solve the action

$$S = \frac{1}{2\pi}\int d^2x\sqrt{-g}e^{-2\phi}\left[R - 4\omega\left(\partial\phi\right)^2 + 4\lambda^2\right], \qquad (1)$$

*Electronic address: LEMOS@ON.BR
†Electronic address: PMSA@MOZART.SI.UALG.PT

where g is the determinant of the 2D metric, R is the curvature scalar, ϕ is a scalar field, λ is a constant, and ω is a parameter. For $\omega = 0$ one obtains the Teitelboim-Jackiw theory, for $\omega = -\frac{1}{2}$ one has planar general relativity, for $\omega = -1$ one has the first-order string theory, and for $\omega = \pm\infty$ one obtains a pure geometrical theory. Equation (1) is a Brans-Dicke type action in two dimensions. A generalized action, where $\phi = \phi(\psi)$, $\omega = \omega(\psi)$, and $\lambda = \lambda(\psi)$ has also been proposed [13]. Here we treat ω and λ as constants.

Varying this equation with respect to g^{ab} and ϕ one gets the equations

$$e^{2\phi}T_{ab} \equiv -2(\omega+1)D_a\phi D_b\phi + D_aD_b\phi - g_{ab}D_cD^c\phi + (\omega+2)g_{ab}D_c\phi D^c\phi - g_{ab}\lambda^2 = 0, \quad (2)$$

$$R - 4\omega D_cD^c\phi + 4\omega D_c\phi D^c\phi + 4\lambda^2 = 0, \quad (3)$$

where D represents the covariant derivative.

In order to find black hole solutions we write the metric in the unitary gauge

$$ds^2 = -e^{2\nu}dt^2 + dx^2, \quad (4)$$

where ν is a function of x and t. If we assume the solution to be static in these coordinates, then Eqs. (2) and (3) reduce to the three equations

$$\phi_{,xx} - (\omega+2)\,\phi_{,x}^{\,2} + \lambda^2 = 0, \quad (5)$$

$$\omega\phi_{,x}^{\,2} + \phi_{,x}\nu_{,x} + \lambda^2 = 0, \quad (6)$$

$$2\omega\phi_{,xx} + \nu_{,xx} - 2\omega\phi_{,x}^{\,2} + 2\omega\phi_{,x}\nu_{,x} + \nu_{,x}^{\,2} - 2\lambda^2 = 0. \quad (7)$$

Note that the Bianchi identities in vacuum imply that 2D spacetimes have only two independent equations; thus we can consider (7) as a spurious equation.

III. THE SOLUTIONS

Equation (5) can be cast in a more elucidative form. If one defines $\Phi = e^{-(\omega+2)\phi}$, then (5) turns into $\Phi_{,xx} = (\omega+2)\lambda^2\Phi$. Thus, the character of the solution (hyperbolic, trigonometric, or linear) will depend on the sign of $(\omega+2)\lambda^2$. We consider the three cases separately: $(\omega+2)\lambda^2 > 0$, $(\omega+2)\lambda^2 < 0$, and $(\omega+2)\lambda^2 = 0$.

A. $(\omega+2)\lambda^2 > 0$

In this case the general solution of Eq. (5) is

$$\phi = -\frac{1}{\omega+2}\ln[A\cosh(\sqrt{(\omega+2)\lambda^2}x) + B\sinh(\sqrt{(\omega+2)\lambda^2}x)], \quad (8)$$

where A and B are constants of integration. Without loss of generality, this solution can be subdivided in three different classes, $A > |B|$, $|A| < |B|$, and $A = |B|$.

1. $A > |B|$

As we will show this case yields eight black holes. Whenever $A > |B|$, solution (8) can be written as

$$\phi = -\frac{1}{\omega+2}\ln\cosh\left(\sqrt{(\omega+2)\lambda^2}x\right) + \phi_0, \quad (9)$$

which is defined for $-\infty < x < \infty$. Inserting this solution in Eq. (6) we obtain the metric

$$ds^2 = -\tanh^2\left(\sqrt{(\omega+2)\lambda^2}x\right) \times \cosh^{\frac{4(\omega+1)}{\omega+2}}\left(\sqrt{(\omega+2)\lambda^2}x\right)dt^2 + dx^2, \quad (10)$$

where the third constant of integration was absorbed by a time rescaling. To clarify some features of the metric it is worth writing it in the Schwarzschild gauge, by defining the radial coordinate r:

$$r = \frac{b^{\frac{\omega+1}{\omega+2}}}{a}\cosh^{\frac{2(\omega+1)}{\omega+2}}\left(\sqrt{(\omega+2)\lambda^2}x\right), \quad (11)$$

with

$$a = \frac{2(\omega+1)\lambda^2}{\sqrt{(\omega+2)\lambda^2}}, \quad (12)$$

and $b = \text{const} > 0$. We draw attention to the fact that the line $-\infty < x < +\infty$ corresponds to the segment $1 < ar/(b^{\frac{\omega+1}{\omega+2}}) < +\infty$; each pair of space inverted points degenerates into just one r. Because of this important circumstance true event horizons will form in cases where black holes were not expected, as it will become clear. Using Eq. (11) the dilaton and metric fields take the form

$$\phi = -\ln(ar)^{2(\frac{1}{\omega+1})}, \quad (13)$$

$$ds^2 = -\left[a^2r^2 - b(ar)^{\frac{\omega}{\omega+1}}\right]dt^2 + \frac{dr^2}{a^2r^2 - b(ar)^{\frac{\omega}{\omega+1}}}, \quad (14)$$

where in Eq. (13) we have set to zero the constant of integration. In Sec. IV we show that the constant b (or ϕ_0) is related with the ADM mass of the solution. Note that $ar = b^{\frac{\omega+1}{\omega+2}}$ gives the radius of the horizon and also that in the unitary gauge the value of the dilaton at the horizon, $x = 0$, is $\phi = \phi_0$.

In the Schwarzschild gauge the solutions are expressed as power laws in the radial variable ar. The cases $\omega = -1$ and $\omega = -2$ seem to have to be handled separately, but in fact one can treat them as limiting cases. As usual, when one has power-law solutions, one also expects exponential and logarithmic solutions. These are precisely given by the cases $\omega = -1$ and $\omega = -2$, respectively.

An important quantity, which signals the appearance of a singularity, is the scalar curvature, given by

$$R = -2\lambda^2\left[\frac{4(\omega+1)^2}{\omega+2} + \frac{2\omega b}{\omega+2}(ar)^{-\frac{\omega+2}{\omega+1}}\right]. \quad (15)$$

Since for different values of b the causal structure does not change, we take here $b = 1$ (which as we shall see in Sec. IV is equivalent to $\phi_0 = 0$). To find the maximal analytical extension of the metric one has to write it in the conformal gauge. The conformal radial coordinate r_* is found from

$$r_* = \int \frac{dr}{a^2r^2 - (ar)^{\frac{\omega}{\omega+1}}}. \quad (16)$$

In the advanced and retarded null coordinates,

$$u = t - r_*, \qquad v = t + r_*, \tag{17}$$

the metric becomes

$$ds^2 = -\left[a^2r^2 - (ar)^{\frac{\omega}{\omega+1}}\right] dudv. \tag{18}$$

The maximal analytical extension is found through the Kruskal coordinates, given by

$$U = -\frac{1}{\sqrt{(\omega+2)\lambda^2}} e^{-\sqrt{(\omega+2)\lambda^2}u}, \tag{19}$$

$$V = \frac{1}{\sqrt{(\omega+2)\lambda^2}} e^{\sqrt{(\omega+2)\lambda^2}v}. \tag{20}$$

In general, the integral in Eq. (16) does not have an analytical expression. Moreover, the maximal analytical extension depends critically on the values of ω. In what follows we consider rational values of ω. There are seven cases which have to be treated separately: $0 < \omega < +\infty$, $\omega = 0$, $-1 < \omega < 0$, $\omega = -1$, $-2 < \omega < -1$, $-\infty < \omega < -2$, and $\omega = \mp\infty$.

(a) $0 < \omega < +\infty$. Within this range of values of ω there is no general analytical solution for the integral in Eq. (16). Thus, one should analyze a typical case. Here we consider $\omega = 1$. The dilaton and the metric in Schwarzschild coordinates are

$$e^{-2\phi} = \sqrt{ar}, \tag{21}$$

$$ds^2 = -\left(a^2r^2 - \sqrt{ar}\right) dt^2 + \frac{dr^2}{a^2r^2 - \sqrt{ar}}, \tag{22}$$

with $a = \frac{4|\lambda|}{\sqrt{3}}$. The conformal radial coordinate can be found from Eq. (16):

$$r_* = \frac{1}{3a} \ln \frac{(\sqrt{ar}-1)^2}{ar + \sqrt{ar} + 1} - \frac{2\sqrt{3}}{3a} \arctan \frac{2\sqrt{ar}+1}{\sqrt{3}}. \tag{23}$$

In the Kruskal coordinates (19) and (20) the metric takes the form

$$ds^2 = -\frac{\sqrt{ar}-1}{|\sqrt{ar}-1|} \sqrt{ar} \left(ar + \sqrt{ar} + 1\right)^{\frac{3}{2}} \times e^{\sqrt{3} \arctan \frac{2\sqrt{ar}+1}{\sqrt{3}}} dUdV, \tag{24}$$

and

$$UV = -\frac{1}{3\lambda^2} \frac{\sqrt{ar}-1}{\sqrt{ar + \sqrt{ar} + 1}} e^{-\sqrt{3} \arctan \frac{2\sqrt{ar}+1}{\sqrt{3}}}. \tag{25}$$

One can now draw the Penrose diagram. For $ar \to +\infty$, one has $UV = -\frac{1}{3\lambda^2} e^{-\frac{\sqrt{3}\pi}{2}}$, which is a vertical hyperbola in the Kruskal picture, i.e., a straight vertical (timelike) line in the Penrose diagram (see Fig. 1). There is a horizon at $ar = 1$, $UV = 0$. We recall that this region, $1 < ar < \infty$, is degenerate in the sense that each point r corresponds to a pair $(-x, x)$ in the unitary gauge. Thus, region I is formed by two distinct triangles glued at $ar = 1$ ($x = 0$). Note now that in Kruskal coordinates the metric is not analytic at $ar = 1$. From Eq. (24) we see that on passing from $ar > 1$ to $ar < 1$, the metric changes sign. Thus in region II, for $ar < 1$, one has to

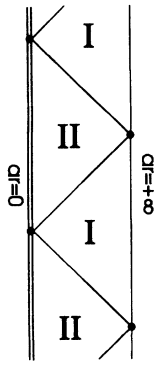

FIG. 1. Penrose diagram for the black hole with $\omega = 1$, $\lambda^2 > 0$, and $A > |B|$ (representative case of $0 < \omega < +\infty$). Region I corresponds to two triangles glued at the horizon. Double lines represent spacetime singularities and simple lines infinities and horizons. This diagram is similar to the extreme four-dimensional Reissner-Nordström black hole diagram.

do $U \to \bar{U} = -U(-u)$ in order that the time direction is vertical. In this patch one has $\bar{U}V = -\frac{1}{3\lambda^2} e^{-\frac{\pi}{2\sqrt{3}}}$ for $ar = 0$. Thus the singularity at $ar = 0$ is also a vertical hyperbola, i.e., is a timelike singularity. To regions I and II there would correspond regions I′ and II′, obtained through the transformation $u \to -u$, $v \to -v$, where the light cones are reversed. However, no trajectory can leave regions I and II to enter regions I′ and II′, and vice versa. For this reason, regions I and II are totally disconnected from I′ and II′. The latter regions are simply replicas of the former, and therefore there is no need to draw them. The future infinity $\mathcal{J}^+$ can be properly defined at $ar \to \infty$. As a matter of fact, there are two disconnected $\mathcal{J}^+$ at $x = \pm\infty$. Observers in these two disconnected regions can only communicate by passing through the horizon $ar = 1$ ($x = 0$) into region II. The solution is indeed a black hole, because the causal past $J^-(\mathcal{J}^+)$ is not the whole diagram. One can now multiply regions I and II *ad infinitum*, obtaining a Penrose diagram which is similar to the one corresponding to the extreme four-dimensional Reissner-Nordström black hole solution. Note, however, that whereas inside the horizon we have here a time-dependent metric, in the extreme Reissner-Nordström case the metric is static. The scalar curvature $R = -\frac{4\lambda^2}{3}\left(8 + \frac{1}{(ar)^{3/2}}\right)$ is negative for all r, which means that gravity has a nonattractive character everywhere. In particular, it gives a timelike singularity inside the horizon.

(b) $\omega = 0$. This case gives the Teitelboim-Jackiw theory, where the scalar curvature is constant, $R = -4\lambda^2$. We have shown [8] that, surprisingly, this constant curvature theory has two important features: first, it admits a black hole, and second, the black hole is free of spacetime singularities. The maximal analytical extension gives a chain of universes connected by timelike wormholes (see Fig. 2 for the Penrose diagram). In Schwarzschild coordinates the dilaton and the metric take the form

$$e^{-2\phi} = ar, \tag{26}$$

$$ds^2 = -\left(a^2r^2 - 1\right) dt^2 + \frac{dr^2}{a^2r^2 - 1}, \tag{27}$$

where $a = \sqrt{2}|\lambda|$. There is again a duplication of region

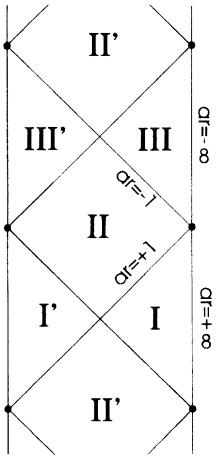

FIG. 2. Penrose diagram for (i) the maximally extended black hole of the Teitelboim-Jackiw theory, $\omega = 0$, $\lambda^2 > 0$, and $A > |B|$, and (ii) the black hole with $\omega = \mp\infty$, $\omega\lambda^2 > 0$, and $A \neq |B|$. Region I is also duplicated. There is an infinite chain of regions, none of them contains a singularity.

I, so that observers at each end of the line $x \to \pm\infty$ can only communicate if they enter through $x = 0$ ($ar = 1$) into region II. An identical duplication applies to region III. The nonsingular character of the whole spacetime is analogous to the behavior of the exact string black hole [5]. The primed regions (I′, II′, and III′) are copies of the unprimed ones.

(c) $-1 < \omega < 0$. For this range of values of ω there is one which is particulary important, $\omega = -\frac{1}{2}$. This gives planar general relativity [11]. The dilaton and metric in Schwarzschild coordinates are given by

$$e^{-2\phi} = a^2 r^2, \tag{28}$$

$$ds^2 = -\left(a^2 r^2 - \frac{1}{ar}\right) dt^2 + \frac{dr^2}{a^2 r^2 - \frac{1}{ar}}, \tag{29}$$

where $a = \sqrt{\frac{2}{3}}|\lambda|$. The scalar curvature is $R = -\frac{4\lambda^2}{3}\left(1 - \frac{1}{(ar)^3}\right)$. There is a spacelike singularity at $ar = 0$, where $R = +\infty$. Inside the horizon the curvature is positive; it passes through zero at the horizon, $ar = 1$, and then becomes negative. Infinity is represented by a timelike line, as in the four-dimensional anti–de Sitter spacetime. The Penrose diagram is given in Fig. 3. Region I can also be duplicated by using the unitary gauge. However, we note that, contrary to the two previous cases, the black hole character of the solution does not depend on this duplication. In other words, solution (28), (29) is by itself a black hole solution. This remark also applies to the black holes described in the following three subsections [III A 1 (d)–III A 1(f)].

(d) $\omega = -1$.

This is the original two-dimensional black hole [2, 3]; it gives the exponential metric. In the Euclideanized version is called the cigar space. From eq. (12) we see that for $\omega = -1$ we lose the scale, $a = 0$. Then, we have to define a new coordinate, $r \to \frac{1}{a}\ln ar$. The dilaton and metric are then

$$e^{-2\phi} = e^{2|\lambda| r}, \tag{30}$$

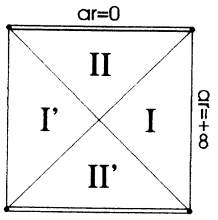

FIG. 3. Penrose diagram for the black hole with $\omega = -\frac{1}{2}$ (representative case of $-1 < \omega < 0$), $\lambda^2 > 0$, and $A > |B|$. Regions I and I′ describe two identical but space-inverted regions. Regions II and II′ describe two identical but time-reversed regions, the black hole and the white hole, respectively. Infinities are timelike lines. The case $\omega = -\frac{1}{2}$ is also a black hole in general relativity.

$$ds^2 = -\left(1 - e^{-2|\lambda r|}\right) dt^2 + \frac{dr^2}{1 - e^{-2|\lambda r|}}. \tag{31}$$

The range of r is $-\infty < r < +\infty$. The scalar curvature is $R = 4\lambda^2 e^{-2|\lambda| r}$, and so there is a singularity at $r \to -\infty$. Spacetime is asymptotically flat for $r \to +\infty$. The Penrose diagram is shown in Fig. 4; it is identical to the Schwarzschild black hole. Two new regions above and below the singularity have been discussed in literature [3, 4].

(e) $-2 < \omega < -1$. Here we analyze two typical cases, $\omega = -\frac{3}{2}$ and $\omega = -\frac{4}{3}$, which give different causal structures.

For $\omega = -\frac{3}{2}$ the dilaton and metric are

$$e^{-2\phi} = \frac{1}{a^2 r^2}, \tag{32}$$

$$ds^2 = -\left(a^2 r^2 - a^3 r^3\right) dt^2 + \frac{dr^2}{a^2 r^2 - a^3 r^3}, \tag{33}$$

with $a = -\sqrt{2}|\lambda|$. In Schwarzschild coordinates the scalar curvature is given by $R = -4\lambda^2\,(1 - 3ar)$. There is a spacelike singularity at $ar \to +\infty$ and a timelike singularity at $ar \to -\infty$. It is useful to change the radial coordinate into $az = \frac{1}{ar}$. The metric then takes the form

$$ds^2 = \frac{1}{a^2 z^2}\left[-\left(1 - \frac{1}{az}\right) dt^2 + \frac{dz^2}{1 - \frac{1}{az}}\right]. \tag{34}$$

We see that in these coordinates the metric is conformal to the Schwarzschild metric. However, at $ar = 0$ ($az = +\infty$) one can continue the solution into the other singularity at $ar = -\infty$. To make the manifold spatially complete one extends it vertically, giving an infinite chain of universes (see Fig. 5).

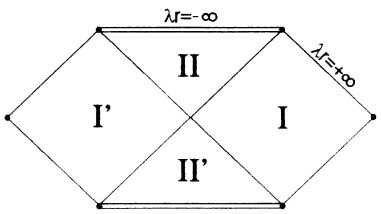

FIG. 4. Penrose diagram for the black hole with $\omega = -1$, $\lambda^2 > 0$, and $A > |B|$. It is similar to the diagram of Fig. 3, but now infinities are null, i.e., is identical to the Schwarzschild diagram. This is the black hole of string theory.

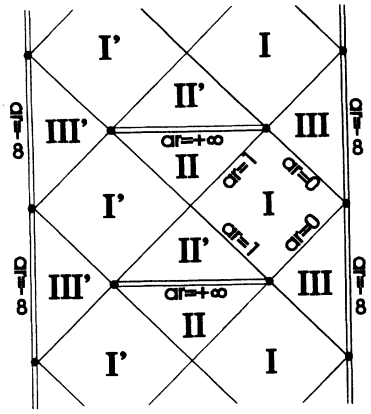

FIG. 5. Penrose diagram for the black hole with $\omega = -\frac{3}{2}$ (representative case of $-2 < \omega < -1$), $\lambda^2 > 0$, and $A > |B|$. There are an infinite chain of universes containing spacelike and timelike singularities.

For $\omega = -\frac{4}{3}$ the dilaton and metric are

$$e^{-2\phi} = \frac{1}{a^3 r^3}, \tag{35}$$

$$ds^2 = -\left(a^2r^2 - a^4r^4\right) dt^2 + \frac{dr^2}{a^2r^2 - a^4r^4}, \tag{36}$$

with $a = -\sqrt{\frac{2}{3}}|\lambda|$ and $R = -\frac{4}{3}\lambda^2[1 - 6(ar)^2]$. Now, the singularities at $ar = \pm\infty$ are both spacelike. The maximal analytical extension is given by a diagram that covers the whole plane (see Fig. 6). These two diagrams cover all possibilities for rational ω.

(*f*) $-\infty < \omega < -2$. As a typical case we take $\omega = -3$. Note that since $\omega + 2 < 0$ we are considering $\lambda^2 < 0$. The dilaton and the metric in Schwarzschild coordinates take the form

$$e^{-2\phi} = \frac{1}{\sqrt{ar}}, \tag{37}$$

$$ds^2 = -\left[a^2r^2 - (ar)^{3/2}\right] dt^2 + \frac{dr^2}{a^2r^2 - (ar)^{3/2}}, \tag{38}$$

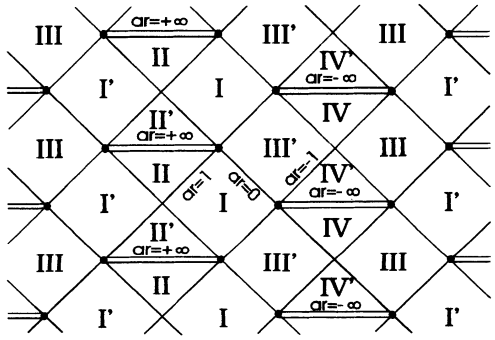

FIG. 6. Penrose diagram for the black hole with $\omega = -\frac{4}{3}$ (also representative of $-2 < \omega < -1$), $\lambda^2 > 0$, and $A > |B|$. There are an infinite chain of universes containing spacelike singularities. The diagram tiles the whole plane.

where $a = 4|\lambda|$. The scalar curvature is $R = 4\lambda^2\left(8 - \frac{3}{\sqrt{ar}}\right)$, which blows up $ar = 0$. The singularity is a null line hidden inside the horizon. The Penrose diagram is shown in Fig. 7.

(*g*) $\omega = \mp\infty$. Taking the limit $\omega \to \mp\infty$ in Eqs. (13) and (14) we obtain

$$\phi = 0, \tag{39}$$

$$ds^2 = -\left(a^2r^2 - ar\right) dt^2 + \frac{dr^2}{a^2r^2 - ar}, \tag{40}$$

with $a = 2|\bar{\lambda}|$, $\bar{\lambda}^2 = \omega\lambda^2 = \text{const} < \infty$. As one can easily see from Eq. (15), the scalar curvature is constant, $R = -8\bar{\lambda}^2$. Thus, we obtain a black hole with a causal structure similar to the $\omega = 0$ case (see Fig. 2) [10]. By adding a Lagrangian matter term to the action (1) one recovers in this limit the $R = T$ theory. In four dimensions the Einstein theory of relativity is also recovered from the Brans-Dicke theory by taking the limit $\omega \to +\infty$. In this sense it is natural to consider the theory given by Eq. (1) in the limit $\omega \to \mp\infty$ as the two-dimensional analogue of general relativity. This is in contrast with the case $\omega = -\frac{1}{2}$, which is identical to vacuum planar general relativity.

Since $\omega \to -\infty$ and $\omega \to +\infty$ have the same solutions one can form a cyclic chain of diagrams, the next one being the typical case $\omega = 1$ (the diagrams with $\omega = -2$ and $\lambda^2 > 0$ or $\lambda^2 < 0$ — Secs. III C 1 and III C 2, respectively — can also enter in this cycle).

2. $|A| < |B|$

This case yields naked singularities, anti–de Sitter spacetime, and also black hole solutions. Whenever $|A| < |B|$, Eq. (8) takes the form

$$\phi = -\frac{1}{\omega + 2} \ln\sinh\left(\sqrt{(\omega + 2)\lambda^2}x\right) + \phi_0, \tag{41}$$

and the metric in the unitary gauge is given by

$$ds^2 = -\coth^2\left(\sqrt{(\omega + 2)\lambda^2}x\right) \times \sinh^{\frac{4(\omega+1)}{\omega+2}}\left(\sqrt{(\omega + 2)\lambda^2}x\right) dt^2 + dx^2. \tag{42}$$

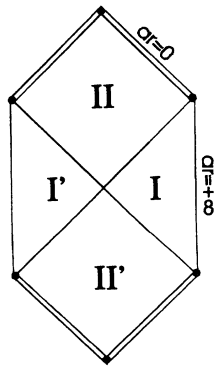

FIG. 7. Penrose diagram for the black hole with $\omega = -3$ (representative case of $-\infty < \omega < -2$), $\lambda^2 < 0$, and $A > |B|$. The singularities are null and the infinities are timelike.

To write Eq. (42) in the Schwarzschild gauge, one defines the radial coordinate r,

$$r = \frac{b^{\frac{\omega+1}{\omega+2}}}{a} \sinh^{\frac{2(\omega+1)}{\omega+2}} \left(\sqrt{(\omega+2)\lambda^2} x \right), \tag{43}$$

where a was defined in Eq. (12) and $b > 0$. Then the dilaton and metric fields take the form

$$\phi = -\ln(ar)^{\frac{1}{2(\omega+1)}}, \tag{44}$$

$$ds^2 = -\left[a^2r^2 + b(ar)^{\frac{\omega}{\omega+1}}\right] dt^2 + \frac{dr^2}{a^2r^2 + b(ar)^{\frac{\omega}{\omega+1}}}, \tag{45}$$

where in Eq. (44) we have set to zero the constant of integration. As for Sec. III A 1 we now divide Sec. III A 2 in seven subsections according to the range of ω. In this section, as in Sec. III A 1, we choose $b = 1$ ($\phi_0 = 0$). Taking $b < 0$ in Eq. (14) is equivalent to Eq. (45).

(a) $0 < \omega < +\infty$. For the typical case $\omega = 1$ the metric takes the form

$$ds^2 = -\left(a^2r^2 + \sqrt{ar}\right) dt^2 + \frac{dr^2}{a^2r^2 + \sqrt{ar}}. \tag{46}$$

The conformal radial coordinate can be found to be

$$r_* = \frac{2}{3a} \ln \frac{\sqrt{ar}+1}{\sqrt{ar - \sqrt{ar}+1}} + \frac{2\sqrt{3}}{3a} \arctan \frac{2\sqrt{ar}-1}{\sqrt{3}}. \tag{47}$$

Defining the null coordinates $u = t - r_*$ and $v = t + r_*$, we find in a Penrose diagram (u, v) that the singularity and infinity are timelike. Since there are no horizons, the singularity is naked (see Fig. 8).

(b) $\omega = 0$. The metric is given by

$$ds^2 = -\left(a^2r^2 + 1\right) dt^2 + \frac{dr^2}{a^2r^2 + 1}. \tag{48}$$

Spacetime is nonsingular and we have here the two-dimensional anti–de Sitter spacetime (see Fig. 9). This is a solution of the Jackiw-Teitelboim theory.

(c) $-1 < \omega < 0$. A typical case is $\omega = -\frac{1}{2}$, which gives a solution of planar general relativity. The metric is

$$ds^2 = -\left(a^2r^2 + \frac{1}{ar}\right) dt^2 + \frac{dr^2}{a^2r^2 + \frac{1}{ar}}. \tag{49}$$

The conformal coordinate is given by

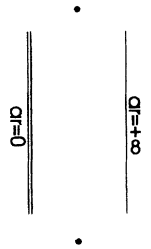

FIG. 8. Penrose diagram for the naked singularity in cases (i) $0 < \omega < +\infty$, $\lambda^2 > 0$, and $|A| < |B|$, (ii) $-1 < \omega < 0$, $\lambda^2 > 0$, and $|A| < |B|$. The two points represent timelike infinity. Spacelike and null infinities are represented by timelike lines.

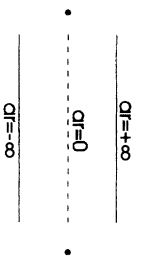

FIG. 9. Penrose diagram for the anti–de Sitter spacetime with $\omega = 0$, $\lambda^2 > 0$, and $|A| < |B|$.

$$r_* = -\frac{1}{6a} \ln \left[\frac{(1+ar)^2}{1 - ar + a^2r^2}\right] + \frac{1}{\sqrt{3}a} \arctan \frac{2ar-1}{\sqrt{3}}. \tag{50}$$

In a Penrose diagram (u, v), one can see that there is a timelike naked singularity. Infinity is also timelike just as in Sec. III A 2 (a) (see Fig. 8).

(d) $\omega = -1$. This is the case provided by string theory. The spacetime has been widely studied [3, 4]. In the Euclideanized version it is called the trumpet spacetime. The Penrose diagram is identical to the four-dimensional Reissner-Nordström naked singularity (see Fig. 10). Spacetime is asymptotically flat.

(e) $-2 < \omega < -1$. For the typical case $\omega = -\frac{3}{2}$ the metric is

$$ds^2 = -\left(a^2r^2 + a^3r^3\right) dt^2 + \frac{dr^2}{a^2r^2 + a^3r^3}. \tag{51}$$

Performing the transformation $ar \to -ar$ we see that this solution coincides with the black hole solution given in Eq. (33) (see Fig. 5 for the Penrose diagram).

For $\omega = -\frac{4}{3}$ the metric is

$$ds^2 = -\left(a^2r^2 + a^4r^4\right) dt^2 + \frac{dr^2}{a^2r^2 + a^4r^4}, \tag{52}$$

which corresponds to the naked singularity shown in Fig. 11.

(f) $-\infty < \omega < -2$. As before, we consider a typical case $\omega = -3$. Then the metric in Schwarzschild coordinates takes the form

$$ds^2 = -\left[a^2r^2 + (ar)^{3/2}\right] dt^2 + \frac{dr^2}{a^2r^2 + (ar)^{3/2}}. \tag{53}$$

The Penrose diagram is shown in Fig. 12. The singularity at $ar = 0$ is represented by null lines.

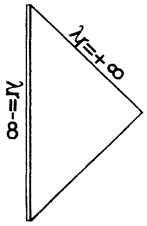

FIG. 10. Penrose diagram for the naked timelike singularity in cases (i) $\omega = -1$, $\lambda^2 > 0$, and $|A| < |B|$, (ii) $\omega = -1$ and $\lambda^2 = 0$ (in this case λ must be dropped out).

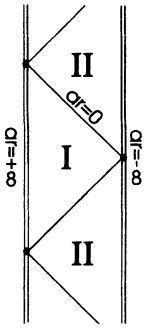

FIG. 11. Penrose diagram for the naked timelike singularity in cases (i) $\omega = -\frac{4}{3}$, $\lambda^2 > 0$, and $|A| < |B|$, (ii) $\omega = -\frac{4}{3}$ and $\lambda^2 = 0$ (in this case a must be replaced by c).

(g) $\omega = \mp\infty$. In the limit $\omega \to \mp\infty$ Eqs. (44) and (45) become

$$\phi = 0, \tag{54}$$

$$ds^2 = -\left(a^2r^2 + ar\right)dt^2 + \frac{dr^2}{a^2r^2 + ar}. \tag{55}$$

This black hole solution coincides with the solution found in Sec. III A 1 (g) (Fig. 2), as it can be seen by redefining $r \to -r$.

3. $A = |B|$

Whenever $A = |B|$, the solution of Eq. (5) takes the form of the linear dilaton

$$\phi(x) = -\frac{\lambda^2}{\sqrt{(\omega+2)\lambda^2}}x + \phi_0. \tag{56}$$

The metric is given by

$$ds^2 = -e^{2ax}dt^2 + dx^2, \tag{57}$$

where the constant a is defined in Eq. (12). For $\omega = -1$ one obtains immediately from Eq. (57) that spacetime is of Minkowski type (see Fig. 13). For $\omega \neq -1$ the dilaton and the metric in the Schwarzschild gauge read

$$\phi = -\ln(ar)^{\frac{1}{2(\omega+1)}}, \tag{58}$$

$$ds^2 = -a^2r^2dt^2 + \frac{dr^2}{a^2r^2}. \tag{59}$$

Taking $b = 0$ in Eq. (14) is equivalent to Eq. (59). This is not a black hole solution with horizons at $ar = 0$ ($x = -\infty$), since there are no duplications. The linear dilaton with $\omega = -2$ is treated in Sec. III C 4. The maximally extended spacetime is shown in Fig. 14. Since

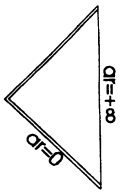

FIG. 12. Penrose diagram for the naked null singularity in cases (i) $-\infty < \omega < -2$, $\lambda^2 < 0$, and $|A| < |B|$, (ii) $-\infty < \omega < -2$ and $\lambda^2 = 0$, (in this case a must be replaced by c).

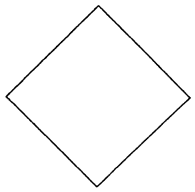

FIG. 13. Penrose diagram for the Minkowski spacetime, corresponding to cases (i) $\omega = -1$, $\lambda^2 > 0$, and $A = |B|$, (ii) $\omega = \mp\infty$ and $\lambda^2 = 0$, (iii) $\omega = 0$ and $\lambda^2 = 0$, (iv) $\lambda^2 = 0$, $\omega = -2$, and $\alpha = 0$.

the scalar curvature is constant, $R = -2a^2$, there are no singularities.

B. $(\omega + 2)\lambda^2 < 0$

The solution of Eq. (5) changes from hyperbolic to trigonometric and is given by

$$\phi = -\frac{1}{\omega+2}\ln\left[C\cos\left(\sqrt{-(\omega+2)\lambda^2}x\right) + D\sin\left(\sqrt{-(\omega+2)\lambda^2}x\right)\right], \tag{60}$$

where C and D are constants of integration. This can be always put in the form

$$\phi = -\frac{1}{\omega+2}\ln\cos\left(\sqrt{-(\omega+2)\lambda^2}x\right) + \phi_0, \tag{61}$$

which is defined for $|x| < \frac{\pi}{2}\frac{1}{\sqrt{-(\omega+2)\lambda^2}}$. The metric in the unitary gauge can be written as

$$ds^2 = -\tan^2\left(\sqrt{-(\omega+2)\lambda^2}x\right) \times \cos^{\frac{4(\omega+1)}{\omega+2}}\left(\sqrt{-(\omega+2)\lambda^2}x\right)dt^2 + dx^2. \tag{62}$$

Schwarzschild coordinates are recovered if we write $\cos^2\left(\sqrt{-(\omega+2)\lambda^2}x\right) = (\bar{a}r)^{\frac{\omega+2}{\omega+1}}b^{-1}$, where $\bar{a} = \frac{2(\omega+1)\lambda^2}{\sqrt{-(\omega+2)\lambda^2}}$. The metric is then

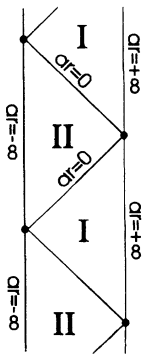

FIG. 14. Penrose diagram for the linear dilaton, appearing in cases (i) $(\omega + 2)\lambda^2 > 0$ ($\omega \neq -1$) and $A = |B|$, (ii) $\lambda^2 = 0$, $\omega = -2$, and $\alpha \neq 0$.

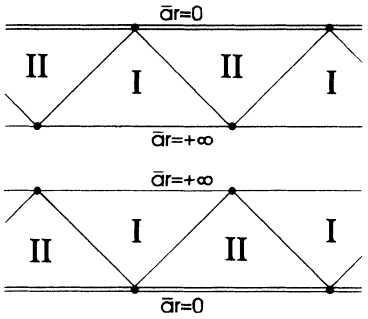

FIG. 15. Penrose diagrams for the cosmological solutions with $0 < \omega < +\infty$ and $\lambda^2 < 0$. There are two disconnected pieces, one having the singularity in the past, the other with the singularity in the future. This diagram can be obtained from the diagram of Fig. 1 by a 90° rotation.

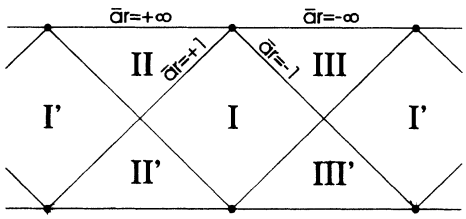

FIG. 16. Penrose diagram for the de Sitter spacetime with (i) $\omega = 0$ and $\lambda^2 < 0$, and (ii) $\omega = \pm\infty$, $\omega\lambda^2 < 0$. This diagram is constructed by horizontally pasting diagrams of the four-dimensional de Sitter spacetime. This diagram can be obtained from the diagram of Fig. 2 by a 90° rotation.

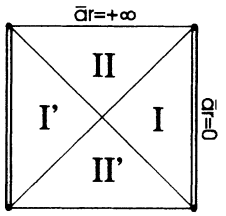

FIG. 17. Penrose diagram for the naked singularity with $-1 < \omega < 0$ and $\lambda^2 < 0$. This diagram can be obtained from the diagram of Fig. 3 by a 90° rotation.

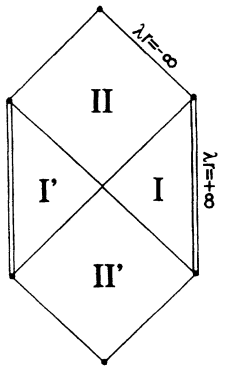

FIG. 18. Penrose diagram for the naked singularity with $\omega = -1$ and $\lambda^2 < 0$. This diagram can be obtained from the diagram of Fig. 4 by a 90° rotation.

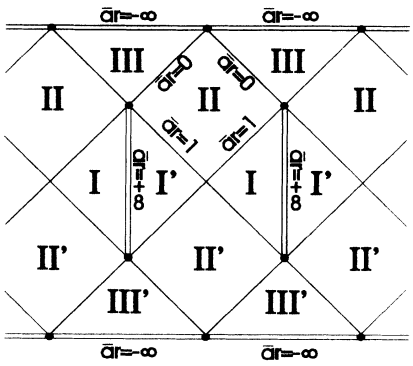

FIG. 19. Penrose diagram for the naked singularity with $\omega = -\frac{3}{2}$ and $\lambda^2 < 0$. Singularities are timelike and spacelike. This diagram can be obtained from the diagram of Fig. 5 by a 90° rotation.

$$ds^2 = -\left[b(\bar{a}r)^{\frac{\omega}{\omega+1}} - \bar{a}^2r^2\right]dt^2 + \frac{dr^2}{b(\bar{a}r)^{\frac{\omega}{\omega+1}} - \bar{a}^2r^2}. \tag{63}$$

As before, we chose $b = 1$ ($\phi_0 = 0$). One can now work the maximal analytical extension. We again divide into seven distinct cases. It is easy to work out that the Penrose diagrams are given by a 90 degrees rotation of Secs. III A 1 (a)–III A 1 (g) (see Figs. 15–21). We now quickly comment on each typical solution, as given in Sec. III A 1.

For $\omega = 1$ there are two different diagrams (see Fig. 15), one with the singularity in the past, the other with the singularity in the future. This is in contrast with Sec. III A 1 (a) (see Fig. 1), where the two disconnected pieces were simply replicas of each other. Region II is duplicated. However, the horizons are cosmological rather than black hole event horizons.

For $\omega = 0$ this solution corresponds to the 2D de Sitter spacetime. The maximal analytical extension is given in

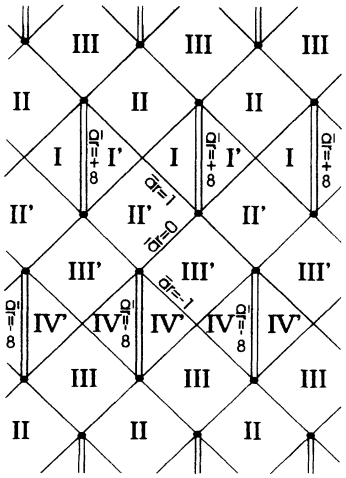

FIG. 20. Penrose diagram for the naked singularity with $\omega = -\frac{4}{3}$ and $\lambda^2 < 0$. Singularities are timelike. The diagram covers the whole plane. This diagram can be obtained from the diagram of Fig. 6 by a 90° rotation.

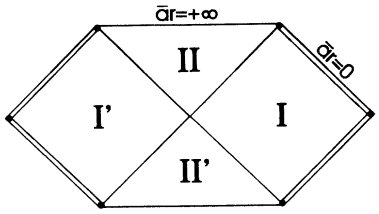

FIG. 21. Penrose diagram for the naked singularity with $-\infty < \omega < -2$ and $\lambda^2 > 0$. This diagram can be obtained from the diagram of Fig. 7 by a 90° rotation.

Fig. 16. Region I is duplicated. The diagram is rather similar to the one obtained by pasting together diagrams of the four-dimensional de Sitter spacetime. Contrarily to the four-dimensional case, the Penrose diagram is not observer dependent.

For $\omega = -1/2$ and $\omega = -1$ the timelike singularities are naked (see Figs. 17 and 18, respectively). Regions I of both diagrams are duplicated. Infinities are spacelike and null for $\omega = -1/2$ and $\omega = -1$, respectively.

For $\omega = -3/2$ and for $\omega = -4/3$ the singularities are naked (see Fig. 19 and 20, respectively).

For $\omega = -3$ the Penrose diagram looks like a Schwarzschild diagram, where the singularities take the place of the Schwarzschild infinities (see Fig. 21).

For $\omega = \mp\infty$ the Penrose diagram is similar to the $\omega = 0$ case (see Fig. 16).

C. $(\omega + 2)\lambda^2 = 0$

Here there are four distinct cases to be considered.

1. $\lambda^2 > 0$ and $\omega = -2$

This solution gives a naked singularity. In the unitary gauge, it is given by

$$\phi = -\frac{\lambda^2}{2}x^2 + \phi_0, \tag{64}$$

$$ds^2 = -\lambda^2 x^2 e^{-2\lambda^2 x^2} dt^2 + dx^2. \tag{65}$$

In Schwarzschild coordinates this gives the logarithmic case mentioned earlier:

$$e^{-2\phi} = -\frac{1}{2|\lambda|r}, \tag{66}$$

$$ds^2 = -4\lambda^2 r^2 \ln(-2|\lambda|r)^{-1} dt^2 + \frac{dr^2}{4\lambda^2 r^2 \ln(-2|\lambda|r)^{-1}}, \tag{67}$$

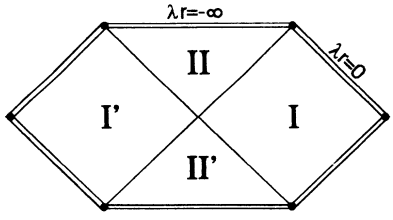

FIG. 22. Penrose diagram for the highly naked singularity with $\omega = -2$ and $\lambda^2 > 0$. The whole frontier of the diagram is singular.

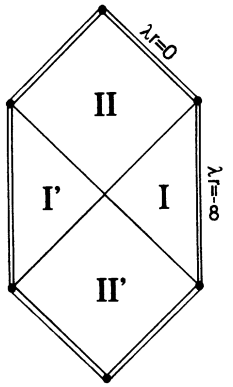

FIG. 23. Penrose diagram for the highly naked singularity with $\omega = -2$ and $\lambda^2 < 0$. The whole frontier of the diagram is singular. This diagram can be obtained from the diagram of Fig. 22 by a 90° rotation.

where we have set to zero in Eq. (66) the constant of integration. It is an interesting example. The scalar curvature is $R = 12\lambda^2 + 8\lambda^2 \ln(-2|\lambda|r)$. Thus, there are singularities at $|\lambda|r = 0$ and $|\lambda|r = -\infty$. The Penrose diagram (see Fig. 22) shows that the whole frontier is singular. The solution can be called a highly naked singularity.

2. $\lambda^2 < 0$ and $\omega = -2$

The Penrose diagram for this naked singularity is given by a 90 degrees rotation of the previous case, Sec. III C 1 (see Fig. 23).

3. $\lambda^2 = 0$ and $\omega \neq -2$

It is straightforward to solve the differential equations (5) and (6) to give

$$\phi = -\frac{1}{\omega + 2}\ln x + \phi_0, \tag{68}$$

$$ds^2 = -x^{\frac{2\omega}{\omega+2}} dt^2 + dx^2. \tag{69}$$

In the Schwarzschild gauge the dilaton and metric read

$$\phi = -\frac{1}{2(\omega + 1)}\ln cr, \tag{70}$$

$$ds^2 = -(cr)^{\frac{\omega}{\omega+1}} dt^2, + \frac{dr^2}{(cr)^{\frac{\omega}{\omega+1}}}, \tag{71}$$

where $c = \frac{2(\omega+1)}{\omega+2}$; we have in Eq. (70) set to zero the constant of integration. For $\omega = -1$ one has to redefine the radial coordinate r as in Sec. III A 1 (d).

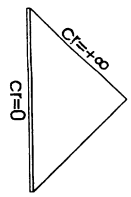

FIG. 24. Penrose diagram for the naked singularity in cases (i) $0 < \omega < +\infty$ and $\lambda^2 = 0$, (ii) $-1 < \omega < 0$ and $\lambda^2 = 0$. Singularities are timelike.

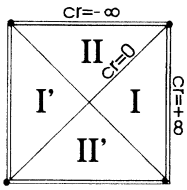

FIG. 25. Penrose diagram for the naked singularity in the case $\omega = -\frac{3}{2}$ and $\lambda^2 = 0$. Singularities are timelike and spacelike. The whole frontier is singular.

From the scalar curvature, $R = \frac{4\omega}{(\omega+2)^2}(cr)^{-\frac{\omega+2}{\omega+1}}$, we conclude that for all values of ω (except $\omega = 0$ and $\omega = \mp\infty$) there are singularities; since horizons are absent, these singularities are naked. For $-\infty < \omega < -2$ the singularities are null (see Fig. 12), and for other values of ω the singularities are spacelike and timelike (see Figs. 10, 11, 24, and 25). For $\omega = 0$ the spacetime is of the Minkowski type (see Fig. 13). In the limit $\omega \to \mp\infty$ the metric (69) goes to the Rindler metric, whose maximal analytical extension yields the Minkowski spacetime.

4. $\lambda^2 = 0$ and $\omega = -2$

The solution is

$$\phi = \alpha x + \phi_0, \tag{72}$$

$$ds^2 = -e^{4\alpha x}dt^2 + dx^2, \tag{73}$$

where α is any constant with the same units as λ. This case yields the linear dilaton solution of $\omega = -2$, which is identical to the case analyzed in Sec. III A 3. The corresponding Penrose diagram for $\alpha \neq 0$ is given in Fig. 14. $\alpha = 0$ gives the Minkowski spacetime.

IV. THE ADM MASSES OF THE SOLUTIONS

A useful and important quantity that appears in the theory of general relativity is the Arnowitt-Deser-Misner (ADM) total mass, which can be defined for isolated black holes. For the two-dimensional black holes one can calculate an analogous quantity. In a static spacetime there is a timelike Killing vector, $\xi^a = \left(\frac{\partial}{\partial t}\right)^a$, which implies the existence of a conserved quantity given by $p^0 = T^0{}_b\xi^b$, where $T^a{}_b$ is given in Eq. (2). The corresponding charge density is a total divergence, $P^0 = \sqrt{-g}p^0$. The total charge is then the analogue of the ADM mass, which can be found through the equation

$$M_{\rm BH} = \int_\infty P^0 d\rho = \int_\infty \sqrt{-g}T^0{}_a\xi^a d\rho, \tag{74}$$

where ρ represents the spatial coordinate at spatial infinity.

In this paper we have worked with the unitary and Schwarzschild gauges. In order to compare the expression for the ADM masses we calculate the integral of Eq. (74) in both gauges.

The idea is to subtract in a correct manner the black hole from the corresponding linear dilaton solution at spatial infinity. In the unitary gauge the linear dilaton solution is given by

$$\bar\phi = -\frac{\lambda^2}{\sqrt{(\omega+2)\lambda^2}}x, \tag{75}$$

$$ds^2 = \bar g_{ab}dx^a dx^b = -e^{2ax}dt^2 + dx^2, \tag{76}$$

where $a = \frac{2(\omega+1)\lambda^2}{\sqrt{(\omega+2)\lambda^2}}$ [see Eqs. (56) and (57)]. At spatial infinity, $x \to \infty$, the black hole solution (9), (10) can be written as

$$\phi = \bar\phi + \varphi, \tag{77}$$

$$g_{ab} = \bar g_{ab} + h_{ab}, \tag{78}$$

where $\bar\phi$ and $\bar g_{ab}$ are the background (linear) dilaton solutions given in Eqs. (75) and (76), and φ and h_{ab} are the fluctuations above the background due to the presence of the black hole. Now, when $x \to \infty$, $\sqrt{-g}T_0{}^0$ goes into

$$\sqrt{-g}T_0{}^0 = \frac{\partial}{\partial x}\left[e^{2\sqrt{(\omega+2)\lambda^2}x}\left(\frac{\partial\varphi}{\partial x} + \frac{\lambda^2}{\sqrt{(\omega+2)\lambda^2}}h_{11}\right)\right]. \tag{79}$$

From (9) and (10) and (75)–(78) we find $\frac{\partial\varphi}{\partial x} = \frac{1}{2}\frac{\lambda^2}{\sqrt{(\omega+2)\lambda^2}}e^{-2(\omega+2)\phi_0}e^{-2\sqrt{(\omega+2)\lambda^2}x}$ and $h_{11} = 0$. Thus, from (74) and (79) one obtains

$$M_{\rm BH} = \frac{1}{2}\frac{\lambda^2}{\sqrt{(\omega+2)\lambda^2}}e^{-2(\omega+2)\phi_0}. \tag{80}$$

In the unitary gauge the mass depends on ϕ_0, the value of ϕ at the horizon $x = 0$ (see also [3]). Following the same procedure for the Schwarzschild gauge we find from Eqs. (13) and (14) and the corresponding linear dilaton solutions (58) and (59) that the total divergence is given asymptotically by

$$\sqrt{-g}T_0{}^0 = \frac{\partial}{\partial r}\left[(ar)^{\frac{2\omega+3}{\omega+1}}a\frac{\partial\varphi}{\partial r} + \frac{1}{4}\frac{a}{\omega+1}(ar)^{\frac{3\omega+4}{\omega+1}}h_{11}\right]. \tag{81}$$

One can easily find that in this case $\varphi = 0$ and $h_{11} = b(ar)^{-\frac{3\omega+4}{\omega+1}}$. Thus, from (74) one obtains

$$M_{\rm BH} = \frac{1}{2}\frac{\lambda^2}{\sqrt{(\omega+2)\lambda^2}}b. \tag{82}$$

In the Schwarzschild gauge the mass of the black hole is related to b, the value of ar at the horizon, since there $b = (ar)^{\frac{\omega+2}{\omega+1}}$. This is what one should expect from experience with the Schwarzschild metric. Through Eqs. (80) and (82) we can relate ϕ_0 and b by

$$b = e^{-2(\omega+2)\phi_0}. \tag{83}$$

Note that expression (80) applies only for the solutions of Sec. III A 1, where $A > |B|$ ($b > 0$). On the other hand, Eq. (82) is valid for $b > 0$, $b < 0$, and $b = 0$. It is now interesting to analyze expression (82) for the several solutions we have obtained.

When $(\omega+2)\lambda^2 > 0$, $\lambda^2 > 0$, and $b > 0$ one has seven different black holes [Secs. III A 1 (*a*)–III A 1(*e*) and III A 1(*g*), Figs. 1–5 and 7, respectively], and the

ADM mass is non-negative, $M_{\rm BH} \geq 0$. For $\omega = 0$ one obtains the mass of the Teitelboim-Jackiw black hole, $M(\omega = 0) = \frac{1}{2}\sqrt{\frac{1}{2}b}|\lambda|$. For $\omega = -\frac{1}{2}$ one obtains the two-dimensional mass (in this case a surface density) of the corresponding planar black hole in general relativity, $M(\omega = -\frac{1}{2}) = \frac{1}{2}\sqrt{\frac{2}{3}b}|\lambda|$. For $\omega = -1$ one obtains Witten's value, $M(\omega = -1) = \frac{1}{2}b|\lambda|$. In the limit $\omega \to \mp\infty$ one obtains the surprising result $M(\omega = \mp\infty) = 0$, although from the causal structure of the solution, Sec. III A 1 (g), one can ascertain the presence of a black hole. When $(\omega + 2)\lambda^2 > 0$, $\lambda^2 > 0$, and $b < 0$, which corresponds to Secs. III A 2 (a)–III A 2 (e) and III A 2 (g) (see Figs. 2, 5, and 8–11), one has solutions with nonpositive mass, some are naked singularities. When $(\omega + 2)\lambda^2 > 0$ and $b = 0$ one has the linear dilaton, and by construction these solutions have zero mass.

When $(\omega + 2)\lambda^2 > 0$, $\lambda^2 < 0$, and $b > 0$, which is Sec. III A 1 (f) (Fig. 6), one has a black hole with negative mass. The corresponding naked singularity, with $b < 0$ (Sec. III A 2 (f), Fig. 12), has positive mass.

When $(\omega + 2)\lambda^2 = 0$ and $\lambda^2 > 0$ (Sec. III C 1, Fig. 22) one has a naked singularity with infinite mass, which is a highly naked singularity. The case $\lambda^2 < 0$ (Sec. III C 2, Fig. 23) gives a highly naked singularity with infinite negative mass. For $\lambda^2 = 0$ (Secs. III C 3 and III C 4, Figs. 10–13 and 24) the ADM mass is zero. Some of these are (massless) naked singularities.

When $(\omega + 2)\lambda^2 < 0$ one has always imaginary masses (see Sec. III B, Figs. 15–21). The ADM mass concept in these cases is meaningless.

V. CONCLUSIONS

We have presented a bewildering variety of solutions which appear in a theory given by action (1)—see Table I for a summary. The theory has two parameters: the cosmological constant λ and the Brans-Dicke parameter ω. For special values of ω some important cases arise. Thus, (i) $\omega \to \mp\infty$ yields a purely geometric two-dimensional theory, (ii) $\omega = 0$ gives the constant curvature theory, (iii) $\omega = -\frac{1}{2}$ is equivalent to (vacuum) planar general relativity, and (iv) $\omega = -1$ is the action one obtains in

TABLE I. This table summarizes all the cases discussed in the text. In the classification column the short names used are WS, with singularity; WOS, without singularity; BH, black hole; NS, naked singularity; and LD, linear dilaton.

Main division	Subsidiary division	Range of ω	Section in the text	Figure number	Classification
		$0 < \omega < +\infty$	III A 1 (a)	Fig. 1	BH WS (Reissner-Nordstrom type)
		$\omega = 0$	III A 1 (b)	Fig. 2	Black hole WOS
		$-1 < \omega < 0$	III A 1 (c)	Fig. 3	Black hole WS
	$A > \lvert B\rvert$	$\omega = -1$	III A 1 (d)	Fig. 4	BH WS (Schwarzschild type)
	($b > 0$)	$-2 < \omega < -1$	III A 1 (e)	Figs. 5,6	Black holes WS
		$-\infty < \omega < -2$	III A 1 (f)	Fig. 7	Black hole WS
		$\omega = \mp\infty$	III A 1 (g)	Fig. 2	Black hole WOS
		$0 < \omega < +\infty$	III A 2 (a)	Fig. 8	Naked singularity
		$\omega = 0$	III A 2 (b)	Fig. 9	Anti-de Sitter spacetime
		$-1 < \omega < 0$	III A 2 (c)	Fig. 8	Naked singularity
$(\omega + 2)\lambda^2 > 0$	$\lvert A\rvert < \lvert B\rvert$	$\omega = -1$	III A 2 (d)	Fig. 10	Naked singularity
	($b < 0$)	$-2 < \omega < -1$	III A 2(e)	Figs. 11,5	Naked singularity and BH WS
		$-\infty < \omega < -2$	III A 2 (f)	Fig. 12	Naked singularity
		$\omega = \mp\infty$	III A 2(g)	Fig. 2	Black hole WOS
	$A = \lvert B\rvert$	$\omega = -1$	III A 3	Fig. 13	Minkowski spacetime (LD)
	($b = 0$)	$\omega \neq -1$	III A 3	Fig. 14	Anti-de Sitter spacetime (LD)
		$0 < \omega < +\infty$	III B	Fig. 15	Future and past spacelike singularities
		$\omega = 0$	III B	Fig. 16	de Sitter spacetime
		$-1 < \omega < 0$	III B	Fig. 17	Naked singularity
$(\omega + 2)\lambda^2 < 0$		$\omega = -1$	III B	Fig. 18	Naked singularity
		$-2 < \omega < -1$	III B	Figs. 19,20	Naked singularities
		$-\infty < \omega < -2$	III B	Fig. 21	Naked singularity
		$\omega = \mp\infty$	III B	Fig. 16	de Sitter spacetime
	$\lambda^2 > 0$	$\omega = -2$	III C 1	Fig. 22	Naked singularity
	$\lambda^2 < 0$	$\omega = -2$	III C 2	Fig. 23	Naked singularity
		$0 < \omega < +\infty$	III C 3	Fig. 24	Naked singularity
		$\omega = 0$	III C 3	Fig. 13	Minkowski spacetime
		$-1 < \omega < 0$	III C 3	Fig. 24	Naked singularity
$(\omega + 2)\lambda^2 = 0$	$\lambda^2 = 0$	$\omega = -1$	III C 3	Fig. 10	Naked singularity
		$-2 < \omega < -1$	III C 3	Figs. 11,25	Naked singularities
		$-\infty < \omega < -2$	III C 3	Fig. 12	Naked singularity
		$\omega = \mp\infty$	III C 3	Fig. 13	Minkowski spacetime
	$\lambda^2 = 0$	$\omega = -2$ ($\alpha = 0$)	III C 4	Fig. 13	Minkowski spacetime (LD)
		$\omega = -2$ ($\alpha \neq 0$)	III C 4	Fig. 14	anti-de Sitter (LD)

string theory by imposing conformal invariance on the string world sheet.

Out of all the solutions the most interesting maybe the black hole solutions with real ADM masses. Depending on the value of ω and λ^2 they have several different causal structures. There are structures similar to (i) the extreme Reissner-Nordstrom ($0 < \omega < +\infty$, $\lambda^2 > 0$, and $A > |B|$), (ii) the nonsingular black holes similar to the exact string theory ($\omega = 0$, $\lambda^2 > 0$, and $A > |B|$; $\omega = \mp\infty$, $\omega\lambda^2 > 0$), (iii) the Schwarzschild black hole analogue ($\omega = -1$, $\lambda^2 > 0$, and $A > |B|$). There are also new structures: (i) $-1 < \omega < 0$, $\lambda^2 > 0$, and $A > |B|$ being a Schwarzschild-like black hole with a timelike infinity, (ii) $-2 < \omega < -1$, $\lambda^2 > 0$, and $A > |B|$ yielding two Penrose diagrams, one of them tiles the whole plane, and (iii) $\omega = -2$ and $\lambda^2 \neq 0$ giving the highly naked singularity. One also finds several naked singularities, obtained by rotating through 90° the above-mentioned diagrams, as well as many other solutions giving naked singularities, anti–de Sitter, de Sitter, and Minkowski spacetimes. Having studied the geometrical structure of this quite general two-dimensional theory, one can now explore its physical consequences, such as thermodynamical properties and black hole evaporation in a fashion similar to what has been done recently [14].

ACKNOWLEDGMENTS

J.P.S.L. acknowledges grants from JNICT (Portugal) and CNPq (Brazil). P.M.S. acknowledges a JNICT (Portugal) Grant No. BIC/776/92.

[1] S. B. Giddings and A. Strominger, Phys. Rev. Lett. **67**, 2930 (1991).
[2] G. Mandal, A. M. Sengupta, and S. R. Wadia, Mod. Phys. Lett. A **6**, 1685 (1991).
[3] E. Witten, Phys. Rev. D **44**, 314 (1991).
[4] R. Dijkgraaf, H. Verlinde, and E. Verlinde, Nucl. Phys. **B371**, 269 (1992).
[5] M. J. Perry and E. Teo, Phys. Rev. Lett. **70**, 2669 (1993); T. Banks and M. O'Loughlin, Phys. Rev. D **48**, 698 (1993).
[6] C. Teitelboim, in *Quantum Theory of Gravity, Essays in Honour of the 60th Birthday of B. DeWitt*, edited by S. Christensen (Hilger, Bristol, 1984), p. 327.
[7] R. Jackiw, in *Quantum Theory of Gravity, Essays in Honour of the 60th Birthday of B. DeWitt*, [6], p. 403.
[8] J. P. S. Lemos and P. M. Sá, "Non-Singular Constant Curvature Two-Dimensional Black Hole," Instituto Superior Técnico Report No DF/IST-8.93, 1993 (unpublished).
[9] R. B. Mann, A. Shiekh, and L. Tarasov, Nucl. Phys. **B341**, 134 (1990); R. B. Mann, Found. Phys. Lett. **4**, 425 (1991).
[10] J. P. S. Lemos and P. M. Sá, Class. Quantum Grav. (to be published).
[11] J. P. S. Lemos, "Two-Dimensional Black Holes and General Relativity," Instituto Superior Técnico Report No. DF/IST-13.93, 1993 (unpublished).
[12] S. W. Hawking and G. F. R. Ellis, *The Large Scale Structure of Spacetime* (Cambridge University Press, Cambridge, England, 1973); R. Wald, *General Relativity* (Chicago University Press, Chicago, 1984).
[13] T. Banks and M. O'Loughlin, Nucl. Phys. **B362**, 649 (1991); C. R. Nappi, in *Topics on Quantum Gravity, Essays in Honor of Louis Witten* (World Scientific, Singapore, 1993), p. 170.
[14] C. G. Callan, S. B. Giddings, J. A. Harvey, and A. Strominger, Phys. Rev. D **45**, R1005 (1992); C. Vaz and L. Witten, "Formation and Evaporation of a Naked Singularity in Two-Dimensional Gravity," University of Algarve Report No. UATP-93/04, 1993 (unpublished).